

## Targeting LRRC15 inhibits metastatic dissemination of ovarian cancer

Upasana Ray <sup>1\*</sup>, Deok-Beom Jung <sup>1,2\*</sup>, Ling Jin <sup>1</sup>, Yinan Xiao <sup>1</sup>, Subramanyam Dasari <sup>3</sup>, Sayantani Sarkar Bhattacharya <sup>1</sup>, Prabhu Thirusangu <sup>1</sup>, Julie K. Staub <sup>1</sup>, Debarshi Roy <sup>1,4</sup>, Bhaskar Roy<sup>5</sup>, S. John Weroha<sup>6</sup>, Xiaonan Hou <sup>6</sup>, James W. Purcell<sup>7</sup>, Jamie N. Bakkum-Gamez<sup>8</sup>, Scott H. Kaufmann<sup>9</sup>, Nagarajan Kannan<sup>10</sup>, Anirban K. Mitra <sup>3\*\*</sup> and Viji Shridhar <sup>1\*\*</sup>

<sup>1</sup>Department of Experimental Pathology and Medicine, Mayo Clinic, Rochester, MN, USA

<sup>2</sup> ASAN Biomedical Research Center, Seoul, S. Korea

<sup>3</sup>Department of Medical and Molecular Genetics, Indiana University School of Medicine, Indianapolis, IN, USA

<sup>4</sup>Alcorn State University, Lorman, MS, USA

<sup>5</sup>Division of Gastroenterology and Hepatology, Mayo Clinic, Rochester, MN, USA

<sup>6</sup>Department of Oncology, Mayo Clinic, Rochester, MN, USA

<sup>7</sup>Department of Oncology Drug Discovery, AbbVie, South San Francisco, CA, USA

<sup>8</sup>Division of Obstetrics and Gynecology, Mayo Clinic, Rochester, MN, USA

<sup>9</sup>Division of Molecular Pharmacology and Experimental Therapeutics, Mayo Clinic, Rochester, MN, USA

<sup>10</sup>Division of Experimental Pathology, Center for Regenerative Medicine, Mayo Clinic, Rochester, MN, USA

\* Both authors contributed equally.

\*\*Correspondence and requests for materials should be addressed to V.S. (email: [shridhar.vijayalakshmi@mayo.edu](mailto:shridhar.vijayalakshmi@mayo.edu))

Running title: LRRC15 is a novel promoter of ovarian cancer metastasis

Table S1

<b>Antibodies</b>	<b>Company</b>	<b>Catalog No.</b>	<b>Ab Dilutions</b>
1. Cleaved PARP1	Cell Signaling Technology, Danvers, MA	cst5625	WB- 1:2000
2. LRRC15	Abcam, MA, U.S.A AbbVie, CA, USA	ab150376	WB- 1:2000 IHC- 1:500
3. PCNA	Santa Cruz Biotechnology, Texas, U.S.A	sc9857	WB- 1:1000
4. ITGB1	R&D	AF1778-SP	WB- 1:1000 IF- 1:100
5. $\beta$ -actin	Gene Tex	GTX629630	WB- 1:1000
6. Cleaved caspase 3	Cell Signaling Technology, Danvers, MA	cst9664	WB- 1:2000
7. Ki67	Cell signaling Technology, Danvers, MA	cst9027	IHC- 1:100
8. GAPDH	Santa Cruz Biotechnology, Texas, U.S.A	sc-47724	WB- 1:1000
9. phospho-FAK Tyr397	Cell signaling Technology, Danvers, MA	cst8556	WB- 1:2000
10. FAK	Cell signaling Technology, Danvers, MA	cst3285	WB- 1:2000
11. Human epithelial specific antigen	Chemicon International, Temecula, CA, U.S.A	CBL251	IF- 1:100
12. Fibroblast activated protein	R&D Systems, Inc., MN, U.S.A	AF3715	IF- 1:100
13. Phalloidin-iFluor 488 Reagent	Abcam, MA, U.S.A	ab176753	IF- 1:500
14. Vinculin	Proteintech, IL, U.S.A	26520-1-AP	IF- 1:500
<b>Reagents</b>	<b>Company</b>	<b>Catalog No.</b>	
1. CellTracker <sup>TM</sup> green (CMFDA)	ThermoFisher Scientific	C2925	
2. Fibronectin	Millipore	FC010	
3. Poly-L-Lysine, 4. Collagen 1A1, 5. Laminin, 6. Vitronectin	Sigma-Aldrich	P4707, C8919, L2020, V8379	
7. 3-(4,5-dimethylthiazol-2-yl)-2,5-diphenyltetrazolium bromide (MTT)	ThermoFisher Scientific	M6494	
8. Antifade mounting medium with DAPI	Vectashield, Burlingame, CA USA	H-1200-10	
9. Protein A/G-agarose beads	Santa Cruz Biotechnology, Texas, U.S.A	sc-2003	
10. Fetal Bovine Serum (FBS)	Biowest	#S181A	
11. 100 $\mu$ g/ml streptomycin and 100U/ml penicillin	Thermo Fisher Scientific	15070063	
12. MCDB-105	Sigma-Aldrich	M6395	
13. Medium-199	Sigma-Aldrich	M4530	
14. DMEM/F12, 15. DMEM (4.5 g/l glucose), 16. RPMI-1640, 17. McCoy's 5A	Thermo Fisher Scientific	#11330032, #11965118, #11875093, #16600082	
18. Ultrosor <sup>TM</sup> G serum substitute	Pall Corporation	15950-017	
19. Hu LRRC15 Recombinant Protein	Sino Biological US Inc.	15786-H02H	

Table S2

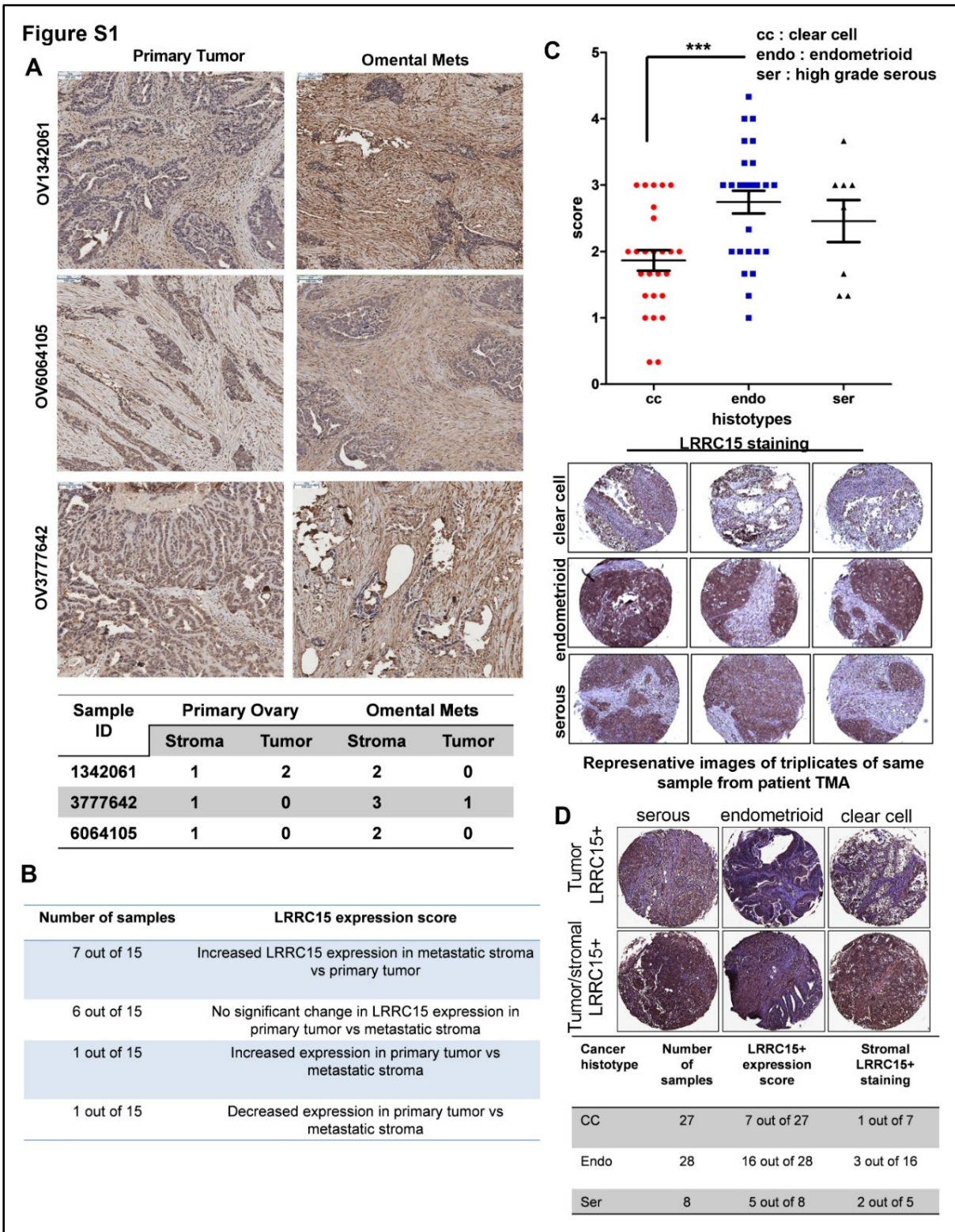
Cell lines	Media	Supplements
OVCAR5/ OVCAR8/ PEO1/ PEO4/ OVCAR4/ OVCAR10/ OV202	RPMI-1640	10% FBS and 1% Pen/Strep
OVCAR7	DMEM (4.5 g/l glucose)	10% FBS, 1% Pen/Strep and insulin (0.25U/ml)
HeyA8MDR/ HeyA8/ Hey1/ COV362/ COV5044	DMEM (4.5 g/l glucose)	10% FBS and 1% Pen/Strep
SKOV3 and derivatives	McCoy's 5A	10% FBS and 1% Pen/Strep
NOF151hTERT/TRS3/TOV21G	MCDB-105: Medium-199 (1:1)	10% FBS and 1% Pen/Strep
Mesothelial LP9/TERT-1 cells	DMEM/F12 (50:50)	10% FBS and 1% Pen/Strep and insulin (0.25U/ml)
Patient-derived ascites	DMEM/F12 (1:1)	15%FBS and 1% Pen/Strep
VOSE and IOSE523 cells	MCDB-105: Medium-199 (1:1)	10% FBS and 1% Pen/Strep

Table S3: Patient details in TMA

<b>sample</b>	<b>morph</b>	<b>stage</b>	<b>grade</b>	<b>sample</b>	<b>morph</b>	<b>stage</b>	<b>grade</b>	<b>sample</b>	<b>morph</b>	<b>stage</b>	<b>grade</b>
<b>1</b>	cc	1C	3	<b>22</b>	cc	3C	3	<b>43</b>	cc	3C	3
<b>2</b>	cc	2C	3	<b>23</b>	cc	1A	3	<b>44</b>	cc	1C	3
<b>3</b>	cc	1C	3	<b>24</b>	ser	3C	4	<b>45</b>	cc	2C	2
<b>4</b>	cc	1	3	<b>25</b>	cc	1C	3	<b>46</b>	endo	3C	3
<b>5</b>	cc	1C	3	<b>26</b>	ser	4	4	<b>47</b>	cc	4	3
<b>6</b>	cc	1C	3	<b>27</b>	endo	3C	3	<b>48</b>	endo	2C	3
<b>7</b>	endo	1C	1	<b>28</b>	endo	3C	4	<b>49</b>	cc	3C	3
<b>8</b>	endo	3C	3	<b>29</b>	endo	1	1	<b>50</b>	cc	3C	3
<b>9</b>	cc	1C	3	<b>30</b>	endo	1B	3	<b>51</b>	endo	3C	4
<b>10</b>	cc	3C	3	<b>31</b>	endo	1A	3	<b>52</b>	endo	1B	2
<b>11</b>	cc	1A	3	<b>32</b>	cc	3B	3	<b>53</b>	cc	3C	4
<b>12</b>	cc	1B	3	<b>33</b>	endo	1A	4	<b>54</b>	endo	3C	2
<b>13</b>	endo	4	4	<b>34</b>	cc	1A	3	<b>55</b>	endo	1A	3
<b>14</b>	endo	3C	3	<b>35</b>	cc	3C	4	<b>56</b>	endo	3C	2
<b>15</b>	ser	3C	4	<b>36</b>	endo	1C	1	<b>57</b>	endo	3C	2
<b>16</b>	endo	1	1	<b>37</b>	ser	3C	4	<b>58</b>	endo	3C	3
<b>17</b>	cc	3C	3	<b>38</b>	cc	4	2	<b>59</b>	cc	1C	3
<b>18</b>	endo	3B	2	<b>39</b>	cc	3C	4	<b>60</b>	endo	1C	2
<b>19</b>	ser	3C	4	<b>40</b>	ser	4	4	<b>61</b>	endo	3C	3
<b>20</b>	endo	1A	2	<b>41</b>	ser	3C	4	<b>62</b>	endo	1C	2
<b>21</b>	endo	1A	1	<b>42</b>	ser	3C	3	<b>63</b>	endo	4	3

Table S4: Human ascites samples

<b>Pt ID</b>	<b>Diagnosis</b>	<b>Stage</b>	<b>Grade</b>	<b>Clinical Information</b>
JM067	High Grade Serous	IIIC	3	Malignant (Fallopian Tube)
AM812	High Grade Serous	IIIC	3	Malignant (Epithelial)
DC738	High Grade Serous	IIIC	3	Malignant (Primary Peritoneal)
KP263	High Grade Serous	IIIC	3	Malignant (Epithelial)
A3626	Serous papillary carcinoma	IIIC	2	Patient recurred after 11 months
A4832	High Grade Serous	late	1	Primary Peritoneal
A7683	High Grade Serous	late	3	Primary Peritoneal
DLD	High Grade Serous	IIIC	-	-



**Figure S1: High expression of LRRC15 is associated with adverse outcome.** (A) Representative IHC analysis of LRRC15 expression in ovarian primary tumors and omental mets in autologous patients were provided. Scale bars 100µm. IHC scores in the PTs and their paired omental mets were represented beneath the image. (B) A cumulative analysis of total number of PTs vs their matched omental mets sample scored for

LRRC15 expression was provided. (C) LRRC15 expression was analyzed in the patient TMA containing 3 different OC histotype (in triplicates for each patient) and plotted. Representative images for the LRRC15 staining in the TMA was provided. (D) LRRC15 expression was scored in stromal and tumor compartments in the TMA and represented.

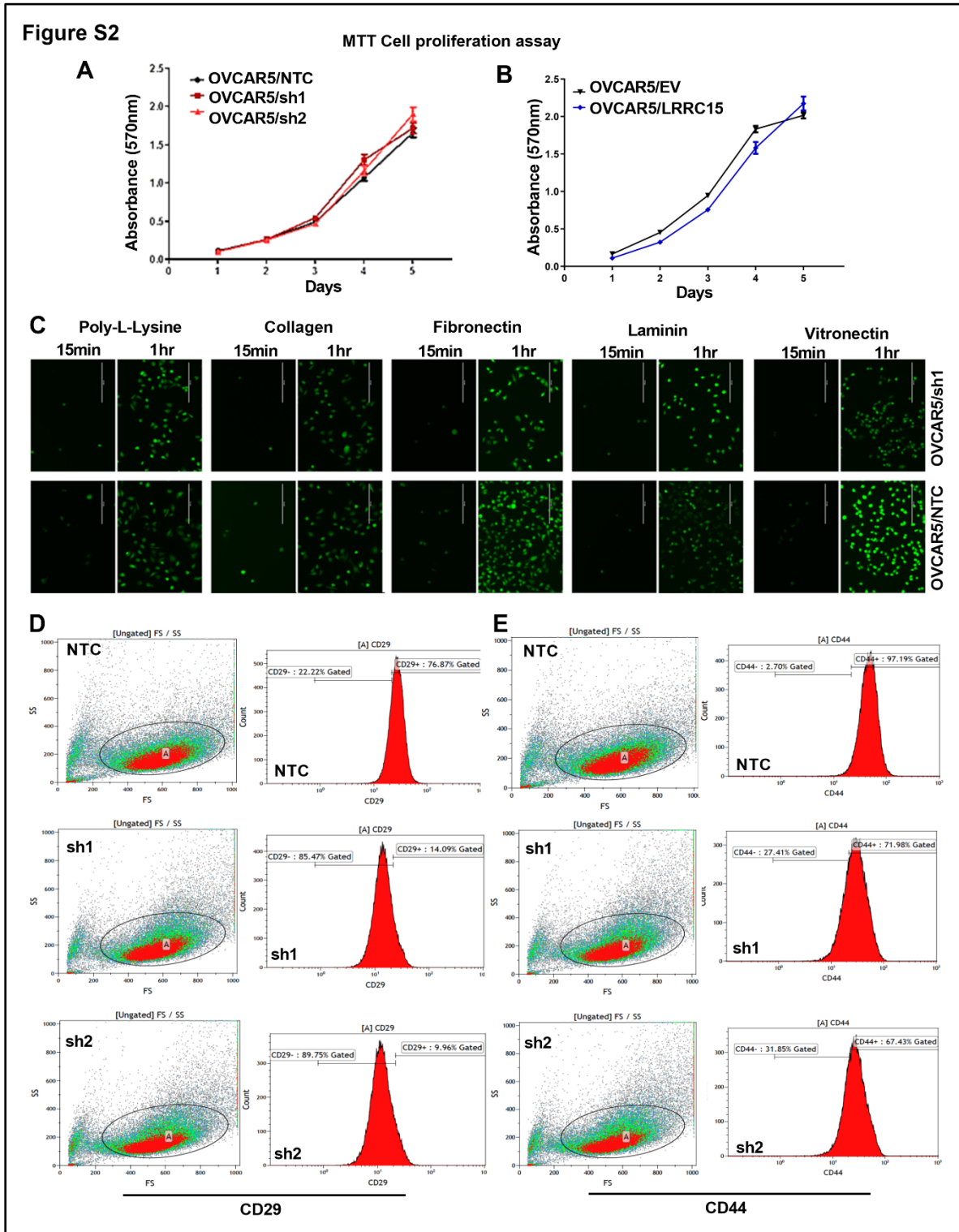


**Figure S2: LRRC15 expression leads to increased adhesion.** (A-B) Cell proliferation assay using MTT was performed and was compared between OVCAR5 NTC and sh1/sh2 LRRC15 KD cells and between OVCAR7 EV and LRRC15 cells. (C) Representative images of CMFDA labeled NTC and sh1 OVCAR5 cells on seeded to the top of the culture dishes that were pre-coated with poly-l-lysine, collagen, fibronectin, laminin and vitronectin respectively was provided after 15mins and 1hr respectively. (D) Gating strategy for the expression analysis of CD29 and (E) CD44 was represented in OVCAR5 NTC control and sh1/sh2 cells.

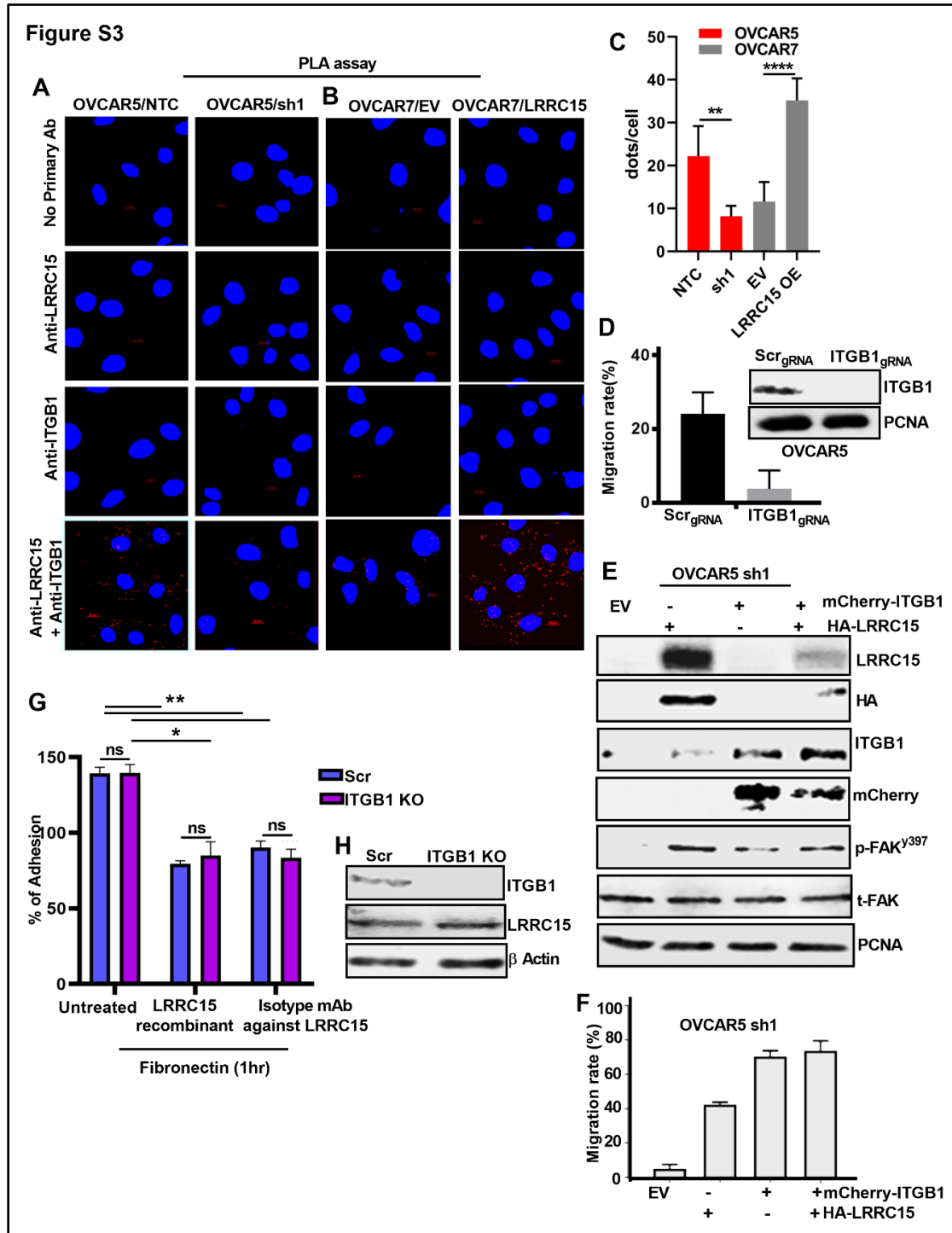


**Figure S3: LRRC15-β1 integrin interaction activates FAK signaling and increased migration in OC cells.**

(A) Proximity ligation assay was performed to score the interaction between ITGB1 and LRRC15 in OVCAR5 NTC and sh1 cells and (B) in OVCAR7 EV and LRRC15 overexpressed cells and representative images were provided. Scale bar 10μm. (C) Red signal dots denoting positive interaction was quantified and the data was provided as dots/cells and mean ± SEM was plotted for each group (\*\*\*\*p<0.0001, \*\*p<0.01). (D) ITGB1 knock out (KO) OVCAR5 cells were generated using CRISPR/Cas9-based approach. Efficient KO was confirmed by western blot. PCNA used as loading control. Scratch wound healing assay was performed in the mentioned cells for 24hrs. Percent cell migration was plotted. (E) OVCAR5 sh1 LRRC15 KD cells were transfected with HA-tagged LRRC15 and mcherry-tagged ITGB1 individually or in combination followed by immunoblot analysis. The p-FAK<sup>y397</sup> and total FAK levels were analyzed. PCNA used as loading control. (F) Under similar condition, wound healing assay was performed with the mentioned transfected cells for 24hrs. Percent cell migration was plotted. (G) Percent cell adhesion was calculated and plotted for the CMFDA labelled scrambled control and ITGB1 KO OVCAR5 cells that still retain LRRC15 expression on FN coated plates before and after pre-blocking the FN binding sites with recombinant LRRC15 protein and M25 monoclonal antibody that is a strong binder of LRRC15. (H) Western blot analysis showing the expression of LRRC15 and ITGB1 in the scrambled control and ITGB1 KO cells.

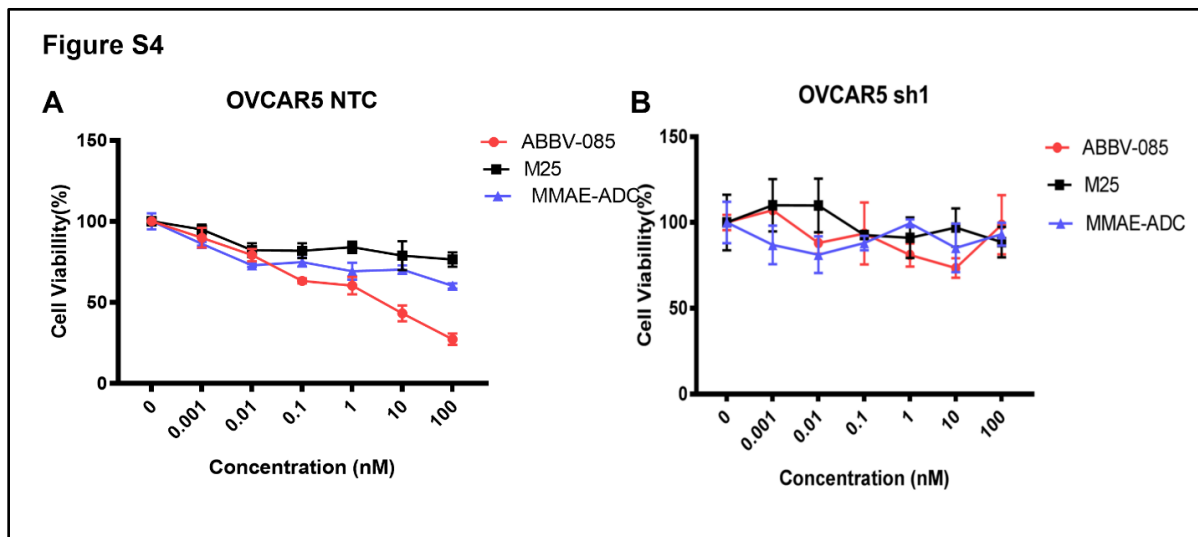


**Figure S4: ABBV-085 inhibits cell viability in the OVCAR5 cells.** (A) Percent cell viability was analyzed in the OVCAR5 NTC and the (B) sh1 LRRC15 KD cells upon treatment with ABBV-085 and the two controls in a dose dependent manner for 24hrs.



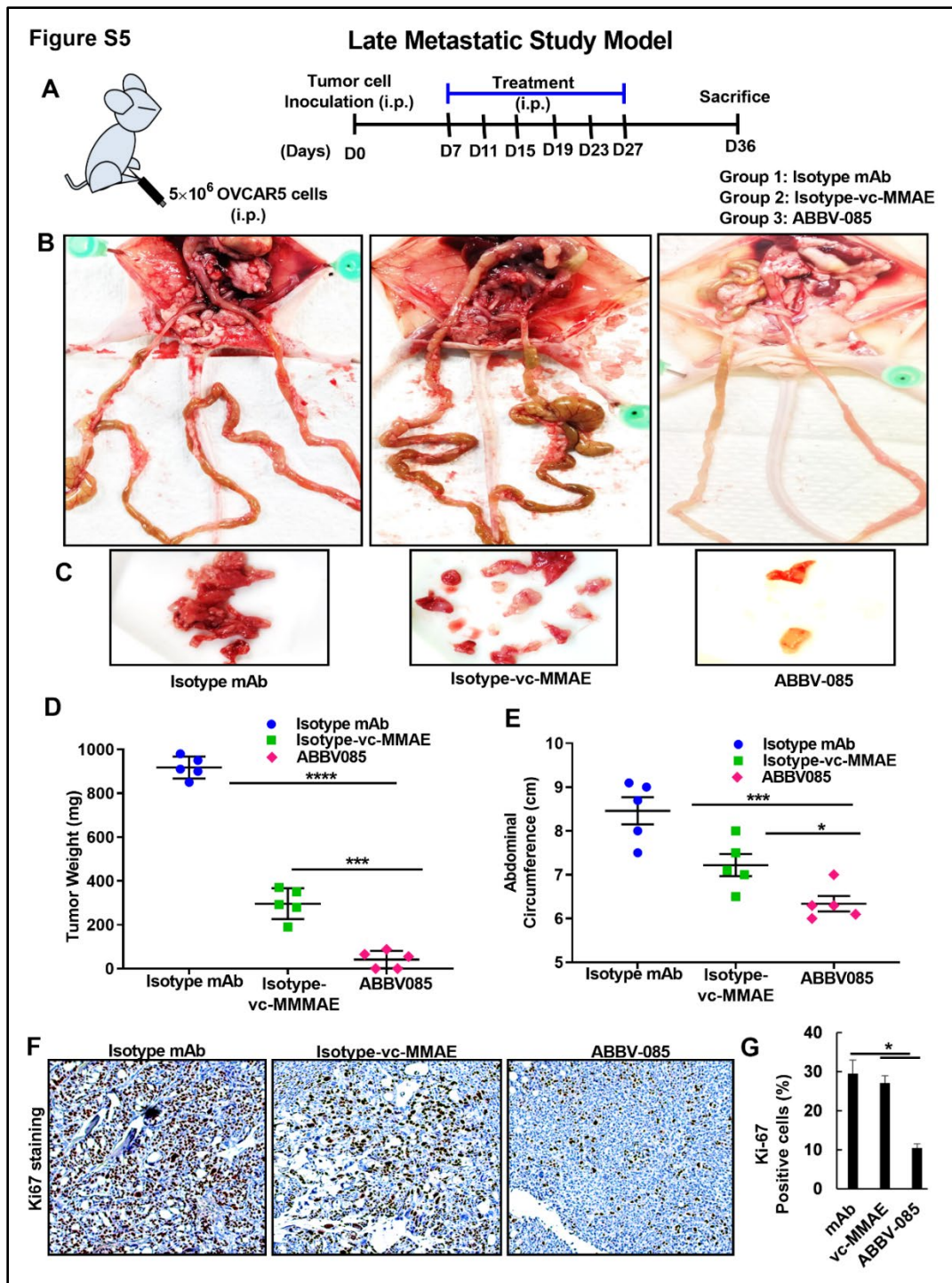


**Figure S5: ABBV-085 inhibits tumor growth in late metastatic model of OVCAR5 xenografts.** (A) Schematic representation of the late metastatic study model in mice OC xenograft was provided. (B) Randomized OVCAR5 tumor-bearing mice were treated as mentioned for 4 weeks and euthanized at day 36. Illustrative images of the mice with the tumor burden and metastatic nodes were shown. (C) Representative images for the tumor burden per mice for the 3 treatment groups were provided. (D) Graphical representation of the excised tumor weights in the 3 treatment cohorts (\*\*\*\* $p < 0.0001$ , \*\*\* $p < 0.001$ ). (E) Abdominal

circumference of each animal measured on the day 36 across the treatment groups (\* $p < 0.05$ , \*\*\* $p < 0.001$ ). (F-G) Ki67 staining in each of the treated group was performed and quantified.

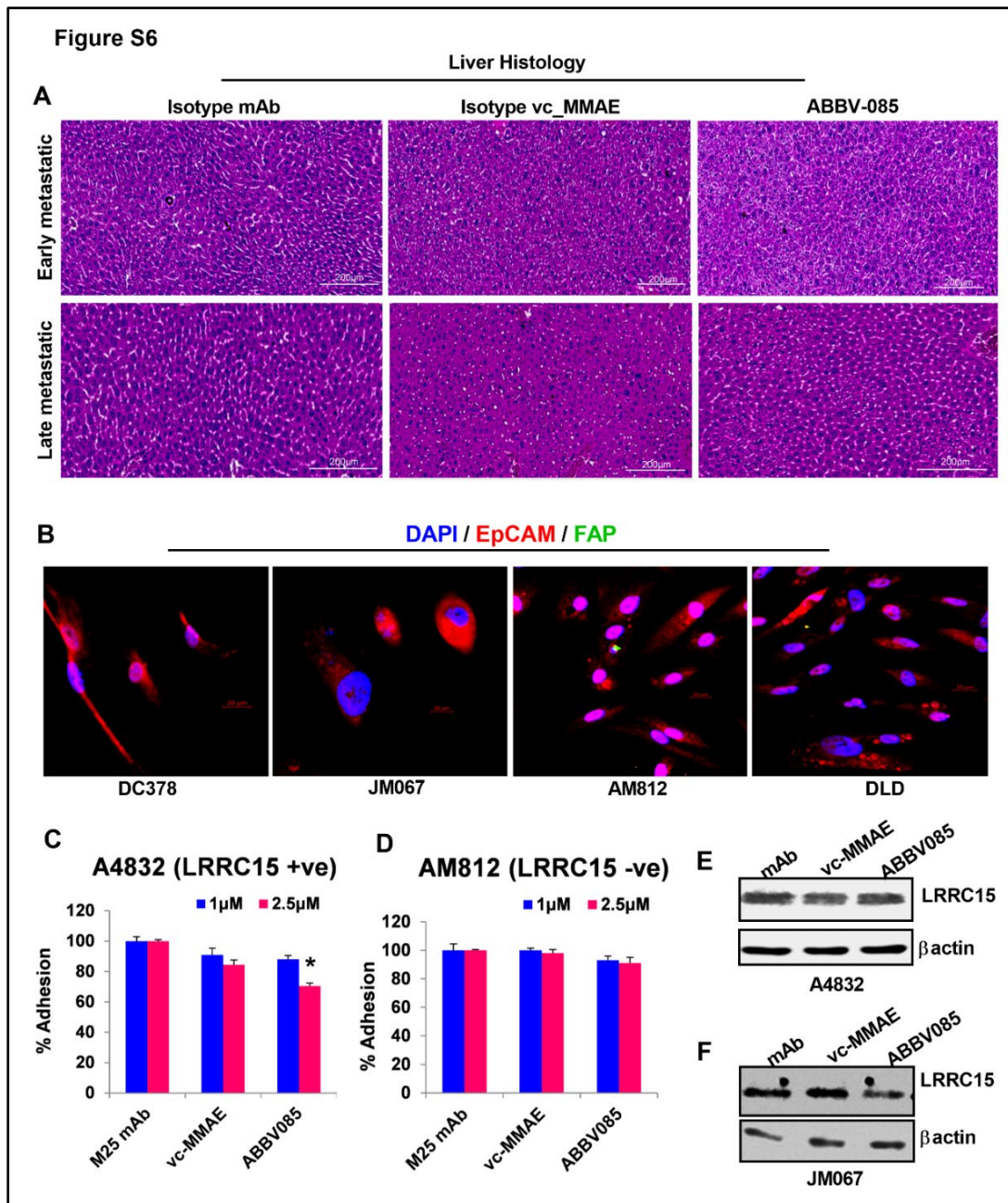


**Figure S6: Treatment with ABBV-085 reduces adhesion in LRRC15-expressing human patient-derived ascites.** (A) H&E staining showing the liver histology in early and late metastatic model of OVCAR5 xenograft was shown in the ABBV-085 treated and drug control groups. (B) Confocal imaging by IF study against the human epithelial specific marker EpCAM (red) and fibroblast specific marker FAP (green) was performed in the patient-derived ascites cells and represented. DAPI was used to stain nucleus. Scale: 20µm. (C) LRRC15

expressing A4832 cells were pre-labeled with CMFDA and then seeded onto the top of the culture dishes that were pre-coated with fibronectin. Percent adhered cells were represented as mean  $\pm$  SEM (\* $p < 0.05$ ). (D) Similar assay was performed with the LRRC15 non-expressing AM812 cells and the percent adhered cells were represented. (E-F) Immunoblot analysis of LRRC15 expression in the A4832 and JM067 ascites cells were performed upon treatment with ABBV-085 and drug controls and presented.  $\beta$  actin was used as loading control.

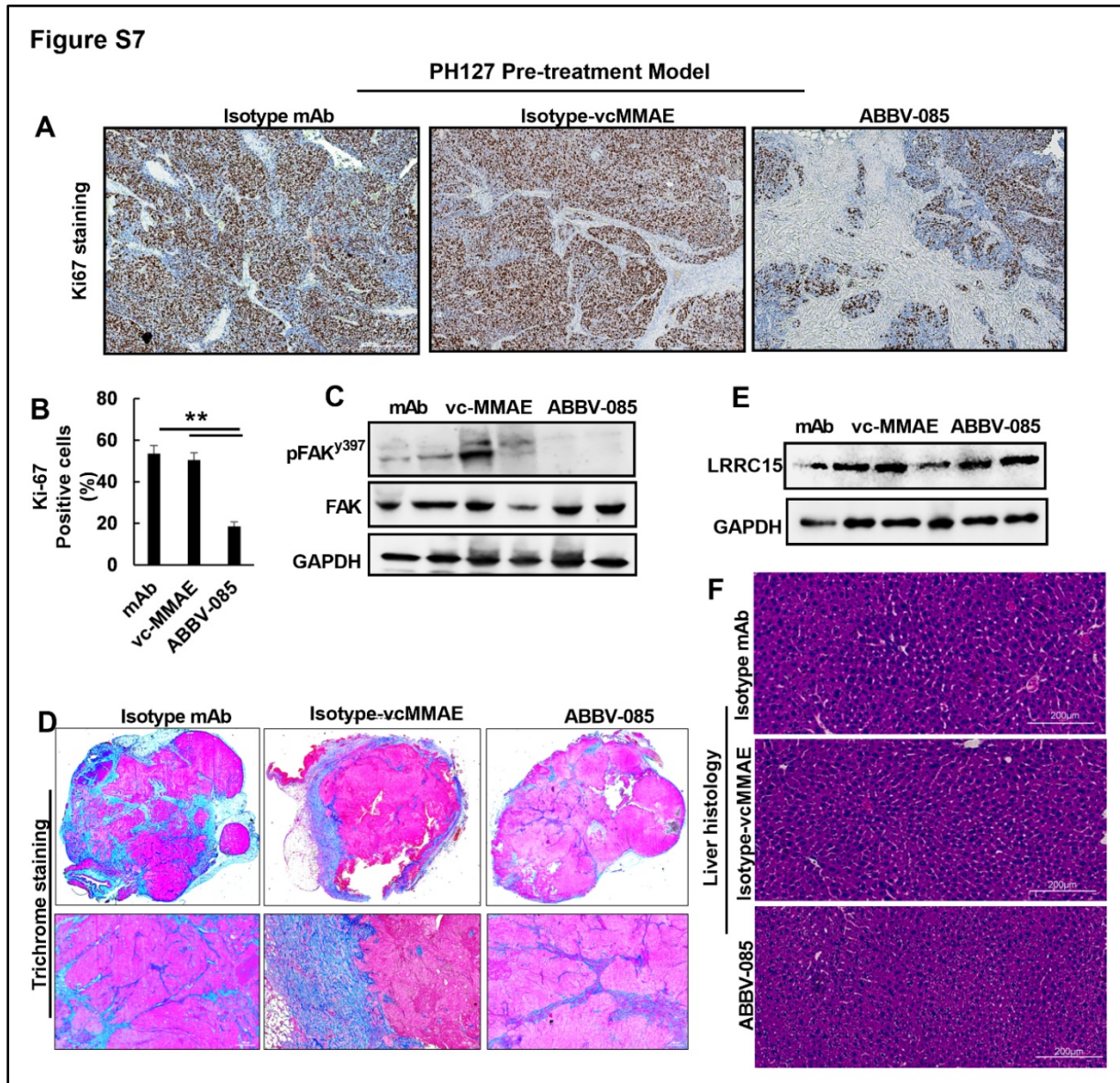


**Figure S7: ABBV-085 therapeutic efficacy in the PH127 PDX xenograft.** (A) Immunostaining showing Ki67 levels in the PH127 early metastatic model tumor sections from mice treated with ABBV-085, mAb control and Isotype-vc-MMAE-E2 drug control. (B) Quantification of Ki67 positive cells was provided

(\*\*p<0.01). (C) Immunoblot analysis of pFAK<sup>y397</sup> and FAK in the xenograft tumors. GAPDH is used as endogenous control. (D) Masson's trichrome staining for ECM infiltration assessment was performed in the xenograft tumors. (E) Western blot analysis for LRRC15 was performed in the xenograft tumors with GAPDH as control. (F) H&E staining showing the liver histology in PH127 PDX xenograft was shown in the ABBV-085 treated and drug control groups.

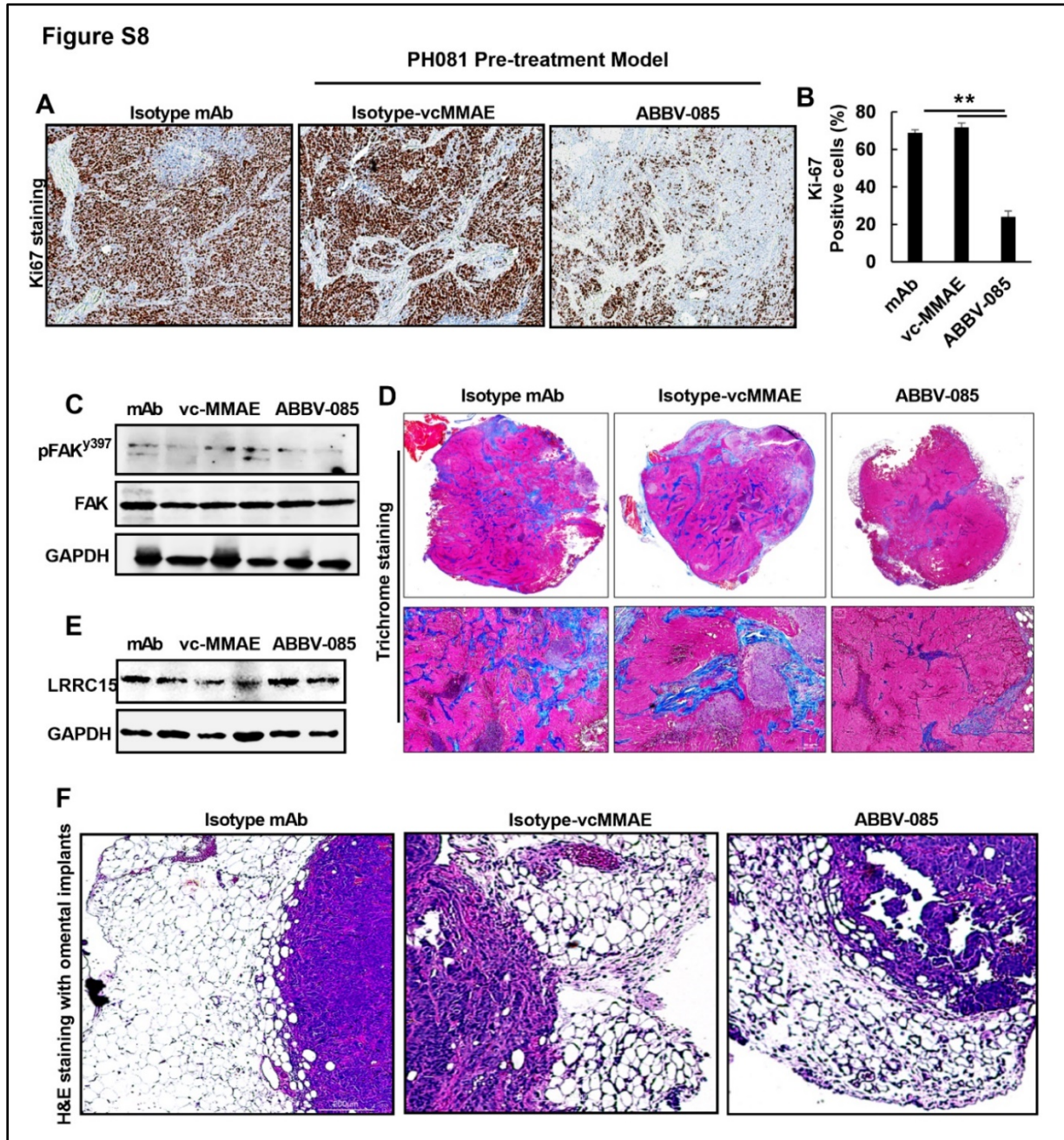


**Figure S8: ABBV-085 therapeutic efficacy in the PH081 PDX xenograft.** (A-B) Immunostaining showing Ki67 levels and quantification in the PH081 early metastatic model tumor sections from the treated groups. (C) Immunoblot analysis of p-FAK<sup>y397</sup> and total FAK in the xenograft tumors. GAPDH is used as endogenous control. (D) Masson's trichrome staining was performed in the xenograft tumors. (E) Western blot analysis for LRRC15 was performed in the xenograft tumors. (F) H&E staining to show the cells in the omental implants were performed in PH081 xenograft treated and control tumor sections.